

Model-independent probes of CP violation in the heavy scalar sector at muon colliders

Qianxi Li ^{a,1}, Ying-nan Mao ^{a,1} and Kechen Wang ^{a,1}

^a*Department of Physics, School of Physics and Mechanics, Wuhan University of Technology, Wuhan 430070, Hubei, China*

E-mail: qianxi_li@whut.edu.cn, ynmao@whut.edu.cn,
kechen.wang@whut.edu.cn

ABSTRACT: We propose a model-independent test of CP violation in the scalar sector. We consider a heavy neutral scalar h_2 with tree-level couplings at the h_2VV and h_2h_1Z vertices (with $V = W^\pm, Z$), alongside the 125 GeV SM-like Higgs boson h_1 . At future muon colliders (MuC), we exploit vector-boson-fusion (VBF) production of h_2 followed by the decay $h_2 \rightarrow Zh_1$. In our framework, observing the single process $VV \rightarrow h_2 \rightarrow Zh_1$ implies both relevant couplings are nonzero, which is sufficient to establish CP violation in the scalar sector. We simulate signal and backgrounds at $\sqrt{s} = 3$ (10) TeV with integrated luminosity $L = 0.9$ (10) ab^{-1} . We then present the expected discovery sensitivities across the (c_2, c_{12}) parameter space (with the coupling parameters c_2 and c_{12} defined in the text) for multiple m_{h_2} hypotheses.

¹Corresponding Author

Contents

1	Introduction	1
2	Model-independent method	3
3	Simulation studies	5
3.1	Simulation setup	5
3.2	Signal and background processes	5
3.3	Analysis strategy	7
3.3.1	Pre-selection	7
3.3.2	Reconstruction	7
4	Results	9
5	Conclusions and discussions	12
A	Additional reconstruction distributions	13
B	Cross sections after each step	14

1 Introduction

CP violation was first discovered in 1964 in the rare decay of the long-lived kaon, $K_L \rightarrow \pi^+\pi^-$ [1]. Additional CP-violating effects have since been measured in meson and baryon systems [2–7]. In the Standard Model (SM), CP violation arises solely from the Kobayashi-Maskawa (KM) mechanism [8], equivalently the complex phase of the Cabibbo-Kobayashi-Maskawa (CKM) matrix [8, 9]. The KM mechanism successfully describes all established CP-violating observables [6, 10, 11]. However, it cannot account for the observed matter–antimatter asymmetry of the Universe [12–14], motivating searches for new sources of CP violation beyond the SM (BSM).

In the SM there is no CP violation originating from the scalar sector. Theoretically, many BSM scenarios introduce additional sources of CP violation, especially in models with an extended scalar sector [15–19]. In such models, the Higgs boson(s) can be CP mixed and thereby exhibit CP-violating interactions. Experimentally, most of these scenarios already face strict constraints from electric dipole moment (EDM) measurements of the electron, neutron, atoms, etc. [20–23], because they typically predict EDMs much larger than in the

SM [24–30]. However, EDMs alone cannot distinguish different CP-violation sources, so direct probes of CP-violating interactions at colliders are also essential.¹

The discovery of the 125 GeV SM-like Higgs boson (denoted h_1 below) at the Large Hadron Collider (LHC) [65–67] marked a turning point in particle physics, making tests of its CP properties crucial for elucidating the Higgs sector. Current data are consistent with a purely CP-even h_1 , but a CP-mixed h_1 is not excluded [47]. In models with an extended scalar sector, there can be additional states $h_{2,3,4,\dots}$ (h_i with $i > 1$), whose possible CP mixing leads to rich collider signatures.

As a representative example, CP violation in the Yukawa sector has been widely studied. For a CP-mixed scalar h_i ($i = 1$ for the 125 GeV state and $i > 1$ for additional scalars) coupled to fermions via

$$\mathcal{L} \supset -h_i \bar{f} (g_S + i g_P \gamma^5) f, \quad (1.1)$$

one typically considers $f = t$ [47–50, 57, 68–86] or $f = \tau$ [32, 51, 52, 87–95], since the spin information of t or τ is imprinted in final-state distributions and is sensitive to the CP nature of h_i . Observation of both CP-even and CP-odd components of h_i would confirm CP violation.

CP violation can also be probed purely in the bosonic sector through interactions of scalars with the massive SM gauge bosons W^\pm and Z , as proposed in Ref. [96]. To employ this method at tree level, at least two scalars must be discovered; the effective interaction can be written as [96]

$$\mathcal{L} \supset \left(\frac{g^2 v}{2} W^{+\mu} W_\mu^- + \frac{g^2 v}{4c_W^2} Z^\mu Z_\mu \right) \left(\sum_i c_i h_i \right) + \sum_{i < j} \frac{c_{ij} g}{2c_W} Z_\mu (h_i \partial^\mu h_j - h_j \partial^\mu h_i), \quad (1.2)$$

where g is the weak gauge coupling, $v = 246$ GeV is the vacuum expectation value (VEV) of the SM Higgs doublet, and $c_W \equiv \cos \theta_W$ is the cosine of the Weinberg angle θ_W . The parameters c_i denote the $h_i VV$ coupling strengths relative to the SM; for the SM-like Higgs h_1 we have $c_1 \simeq 1$. For any two distinct scalars h_i and h_j , the quantity $K \equiv c_i c_j c_{ij}$ serves as a measure of CP violation [19, 96, 97]. Since nonzero c_i implies a CP-even component in h_i , and nonzero c_{ij} implies that h_i and h_j contain components of opposite CP number, $K \neq 0$ is a sufficient condition to establish CP violation. Recent collider studies employing this method include Refs. [43, 46, 96, 98].

In this paper we focus on CP violation in the pure bosonic sector following Ref. [96]. Ref. [96] considers a light extra scalar h_2 and prospects at a Higgs factory with $\sqrt{s} = 250$ GeV (e.g., CEPC [99–101]), however, light new states are already tightly constrained; we therefore study a heavy h_2 scenario with $m_{h_2} \sim \mathcal{O}(\text{TeV})$. We consider future muon colliders (MuC) [102–108] with \sqrt{s} up to 10 TeV, where TeV-scale scalars are kinematically accessible. Specifically, we study vector-boson-fusion (VBF) production with $h_2 \rightarrow Zh_1$, i.e., $VV \rightarrow h_2 \rightarrow Zh_1$ with $V = W^\pm, Z$. Observation of this single process implies $c_2 \neq 0$ and $c_{12} \neq 0$ simultaneously, thereby probing CP violation in the scalar sector.

¹These two complementary avenues have generated a rich phenomenology of CP violation in BSM scenarios; see, e.g., Refs. [31–64] for details.

The paper is organized as follows. In Sec. 2 we describe our model-independent method to search for CP violation. In Sec. 3 we present the simulation setup and analysis. In Sec. 4 we show the results. Conclusions are given in Sec. 5, with additional details in the Appendices A and B.

2 Model-independent method

Assuming that a heavy neutral scalar h_2 has been discovered, following Ref. [96] we write the effective interaction as

$$\mathcal{L} \supset \left(\frac{g^2 v}{2} W^{+\mu} W_{\mu}^{-} + \frac{g^2 v}{4c_W^2} Z^{\mu} Z_{\mu} \right) (c_1 h_1 + c_2 h_2) + \frac{c_{12} g}{2c_W} Z_{\mu} (h_1 \partial^{\mu} h_2 - h_2 \partial^{\mu} h_1). \quad (2.1)$$

Since $c_1 \simeq 1$, CP violation can be confirmed if both c_2 and c_{12} are nonzero, as discussed above. It is then natural to study the VBF processes $VV \rightarrow h_2 \rightarrow Zh_1$ with $V = W^{\pm}, Z$ at MuC, whose Feynman diagrams are shown in Fig. 1.

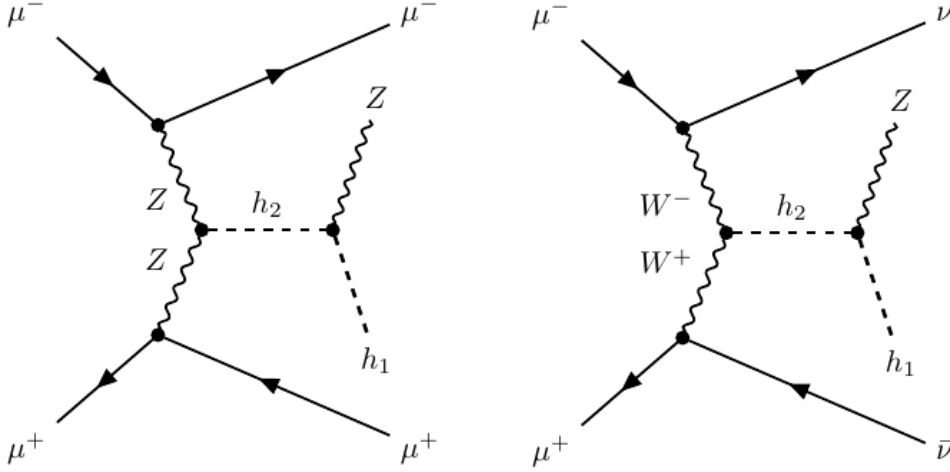


Figure 1: Feynman diagrams for the VBF processes $VV \rightarrow h_2 \rightarrow Zh_1$ (with $V = W^{\pm}, Z$).

In these processes, h_2 is produced via the $h_2 VV$ vertex, giving a total cross section $\sigma_{VV \rightarrow h_2} \propto c_2^2$, and subsequently decays through the $h_1 h_2 Z$ vertex with branching ratio $\text{Br}_{h_2 \rightarrow Zh_1} \equiv \Gamma_{h_2 \rightarrow Zh_1} / \Gamma_{h_2} \propto c_{12}^2 / \Gamma_{h_2}$, where Γ_{h_2} denotes the total decay width of h_2 . If either $c_2 = 0$ or $c_{12} = 0$, then $\sigma_{VV \rightarrow h_2} \cdot \text{Br}_{h_2 \rightarrow Zh_1} = 0$ and the process is absent; conversely, the observation of such a process implies $c_2 c_{12} \neq 0$ and hence CP violation in the scalar sector. We compute $\sigma_{VV \rightarrow h_2}$ at future MuC with $\sqrt{s} = 3$ and 10 TeV, respectively, using `MadGraph5_aMC@NLO` (v3.6.2) [109], and show its dependence on m_{h_2} in Fig. 2 (left). For given m_{h_2} and \sqrt{s} , the cross section of $W^+ W^-$ -fusion is about an order larger than that of ZZ -fusion, which means that $W^+ W^-$ -fusion is the dominant process. For $c_2 \simeq 0.2$ which is a typical benchmark point in the following analysis, the total cross section $\sigma_{VV \rightarrow h_2} \propto c_2^2$ can reach at most $\mathcal{O}(1-10)$ fb in the mass region considered in this work, and decreases quickly as m_{h_2} increases.

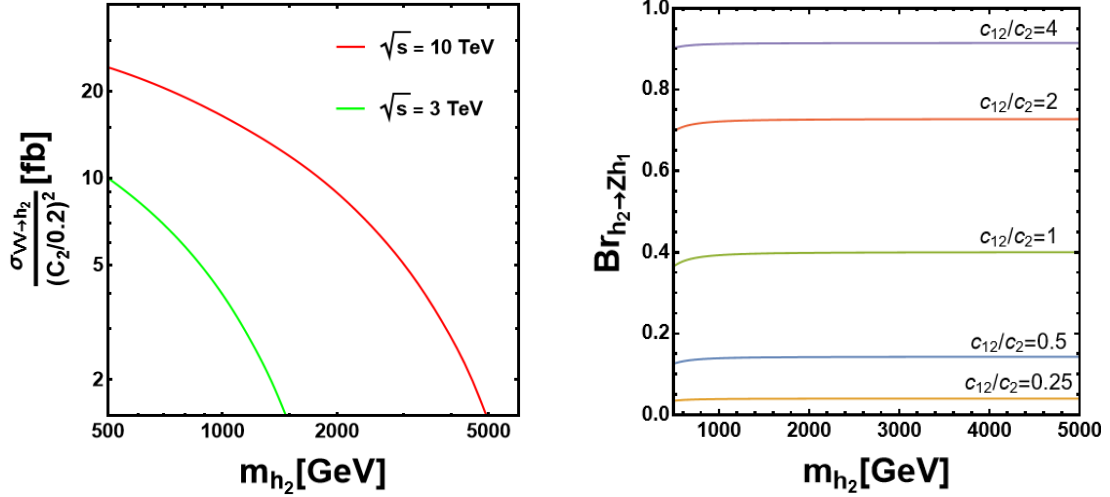


Figure 2: Left: total cross sections σ of $VV \rightarrow h_2$ at MuC with $\sqrt{s} = 3$ and 10 TeV as a function of m_{h_2} . Right: $\text{Br}_{h_2 \rightarrow Zh_1}$ as a function of m_{h_2} for different c_{12}/c_2 .

We assume that Eq. (2.1) contains all the interactions related to h_2 , and thus h_2 decays only through the following three channels: $h_2 \rightarrow Zh_1$, $h_2 \rightarrow ZZ$, and $h_2 \rightarrow W^+W^-$. The branching ratio for the decay channel $h_2 \rightarrow Zh_1$ is defined as

$$\text{Br}_{h_2 \rightarrow Zh_1} \equiv \frac{\Gamma_{h_2 \rightarrow Zh_1}}{\Gamma_{h_2}} = \frac{\Gamma_{h_2 \rightarrow Zh_1}}{\Gamma_{h_2 \rightarrow Zh_1} + \Gamma_{h_2 \rightarrow W^+W^-} + \Gamma_{h_2 \rightarrow ZZ}}, \quad (2.2)$$

where the partial decay widths are given by [19, 110, 111]

$$\Gamma_{h_2 \rightarrow W^+W^-} = \frac{m_{h_2}^3 c_2^2}{16\pi v^2} \sqrt{1 - \frac{4m_W^2}{m_{h_2}^2}} \left(1 - \frac{4m_W^2}{m_{h_2}^2} + \frac{12m_W^4}{m_{h_2}^4} \right), \quad (2.3)$$

$$\Gamma_{h_2 \rightarrow ZZ} = \frac{m_{h_2}^3 c_2^2}{32\pi v^2} \sqrt{1 - \frac{4m_Z^2}{m_{h_2}^2}} \left(1 - \frac{4m_Z^2}{m_{h_2}^2} + \frac{12m_Z^4}{m_{h_2}^4} \right), \quad (2.4)$$

$$\Gamma_{h_2 \rightarrow Zh_1} = \frac{m_{h_2}^3 c_{12}^2}{16\pi v^2} f^3 \left(\frac{m_Z^2}{m_{h_2}^2}, \frac{m_{h_1}^2}{m_{h_2}^2} \right). \quad (2.5)$$

Here $m_{h_1, h_2, Z, W}$ denote the corresponding particle masses, and the function

$$f(x, y) \equiv \sqrt{1 + x^2 + y^2 - 2x - 2y - 2xy}. \quad (2.6)$$

If $m_{h_2} \gg m_{h_1, W, Z}$, the total decay width of h_2 approximately behaves as

$$\Gamma_{h_2} \simeq (493 c_2^2 + 329 c_{12}^2) \left(\frac{m_{h_2}}{1 \text{ TeV}} \right)^3 \text{ GeV}. \quad (2.7)$$

Numerically, Fig. 2 (right) shows $\text{Br}_{h_2 \rightarrow Zh_1}$ as a function of m_{h_2} for different ratios c_{12}/c_2 . The branching ratio is sensitive to c_{12}/c_2 but only weakly dependent on m_{h_2} . In particular, in the limit $m_{h_2} \gg m_{h_1, W, Z}$, we have approximately

$$\text{Br}_{h_2 \rightarrow Zh_1} \simeq \frac{2(c_{12}/c_2)^2}{2(c_{12}/c_2)^2 + 3}, \quad (2.8)$$

which is nearly independent on m_{h_2} .

3 Simulation studies

3.1 Simulation setup

In this work, we study the VBF processes $VV \rightarrow h_2 \rightarrow Z(\rightarrow \ell^+\ell^-)h_1(\rightarrow b\bar{b})$ with $V = W^\pm, Z$ and $\ell = e, \mu$ at MuC, assuming that a heavy h_2 has already been discovered. The effective interaction in Eq. (2.1) is implemented with `FeynRules` (v2.0) [112] to produce a UFO model, which we load in `MadGraph5_aMC@NLO` (v3.6.2) [109] to simulate the $\mu^-\mu^+$ collisions, and generate events for the whole processes of both signal and backgrounds. Event generation is then interfaced to `PYTHIA` 8.3 [113] for parton showering and hadronization. Detector response is simulated with `Delphes` 3.4.2 [114] using a muon-collider configuration card.

An absorber is installed at MuC to mitigate beam-induced backgrounds (BIB), so only objects within $10^\circ < \theta < 170^\circ$ are reconstructed, where θ denotes the polar angle with respect to the z -axis (the initial μ^- beam direction) [115–118]. Objects produced in the very forward/backward regions are absorbed and thus considered to be undetected in this study.

We must treat jets in this work, because the signal we consider here includes two b -jets, and we must also consider the background processes including b -jets or light jets which are mis-tagged as b -jets. For jet reconstruction, we use the algorithm of “VLCjetR05N2” [119–122]. The double- b -tagging efficiency is approximately 0.8, while the probability to mis-tag non- b -jets as two b -jets can reach about $\mathcal{O}(10^{-2})$ [122].

3.2 Signal and background processes

At future MuC, we target the VBF processes $VV \rightarrow h_2 \rightarrow h_1Z$ to search for CP violation in the scalar sector, as shown in Fig. 1. For most events from the ZZ -fusion topology (left panel of Fig. 1), the scattered muons emerge at very small polar angles and low transverse momentum p_T , and therefore are outside the detector acceptance. We select $Z \rightarrow \ell^-\ell^+$ (with $\ell = e, \mu$) and $h_1 \rightarrow b\bar{b}$. For W^+W^- -fusion, the final state contains two energetic neutrinos, which are undetectable; while for ZZ -fusion, the final state contains two energetic μ^\pm , which appear in the very forward/backward region in most events, and thus cannot be detected as well. Hence we generate the two VBF topologies together, in which the final state contains large missing energy, two opposite-charge, same-flavor leptons, and two b -tagged jets.

The signal-generation cross section σ_{sig} scales with a parameter

$$\kappa \equiv c_2^2 \cdot \text{Br}_{h_2 \rightarrow Zh_1}, \quad (3.1)$$

and thus depends on m_{h_2} , c_2 , and c_{12} . In the limit $m_{h_2} \gg m_{h_1, W, Z}$, we have approximately $\kappa \simeq \frac{2c_2^2 c_{12}^2}{3c_2^2 + 2c_{12}^2}$ based on the results in Eqs. (2.3) - (2.5). For the chosen final state, the cross section is also proportional to the SM branching fractions [6]

$$\text{Br}_{Z \rightarrow \ell^-\ell^+} = 0.033647, \quad \text{and} \quad \text{Br}_{h_1 \rightarrow b\bar{b}} = 0.5824. \quad (3.2)$$

Global fits to the 125 GeV Higgs signal strengths data and (approximate) custodial symmetry imply $c_2^2 + c_{12}^2 \lesssim 0.1$ [47], and thus we choose the parameter region $c_2 \leq 0.2$ and $c_{12} \leq 0.2$ as benchmarks². Direct LHC searches for a heavy scalar decaying to ZZ final state further constrain c_2 for $m_{h_2} \lesssim 700$ GeV [123]; and thus we choose all the benchmark points with $m_{h_2} \gtrsim 700$ GeV due to the consistency with LHC bounds.

We consider two center-of-mass energies of the $\mu^- \mu^+$ collisions, $\sqrt{s} = 3$ and 10 TeV. The corresponding integrated luminosities are $L = 0.9$ and 10 ab^{-1} , respectively [102]. To generate the signal samples, we choose the following benchmark points:

$$m_{h_2} \in \begin{cases} \{700, 1000\} \text{ GeV}, & (\text{for } \sqrt{s} = 3 \text{ TeV}); \\ \{700, 1000, 1500, 2000, 3000, 4500\} \text{ GeV}, & (\text{for } \sqrt{s} = 10 \text{ TeV}). \end{cases} \quad (3.3)$$

All signal events are generated with the parameter choice $c_2 = c_{12} = 0.2$, which leads to the largest allowed width of h_2 , to ensure that our search strategy works in the whole parameter region with $(c_2, c_{12}) \leq 0.2$.

Given the final state containing undetected forward/backward muons or neutrinos, two opposite-charge same flavor leptons, and two b -tagged jets (including the mis-tagged non- b -jets), we consider four main backgrounds:

- (i) $VV \rightarrow h_2 \rightarrow Z(\rightarrow \ell^- \ell^+) Z(\rightarrow jj)$ which is a typical BSM background process, labeled “b1” with cross section σ_{b1} . Here σ_{b1} scales with a parameter

$$\xi \equiv c_2^2 \cdot \text{Br}_{h_2 \rightarrow ZZ}, \quad (3.4)$$

where

$$\text{Br}_{h_2 \rightarrow ZZ} \equiv \frac{\Gamma_{h_2 \rightarrow ZZ}}{\Gamma_{h_2}} = \frac{\Gamma_{h_2 \rightarrow ZZ}}{\Gamma_{h_2 \rightarrow Zh_1} + \Gamma_{h_2 \rightarrow W^+ W^-} + \Gamma_{h_2 \rightarrow ZZ}}. \quad (3.5)$$

In the limit $m_{h_2} \gg m_{h_1, W, Z}$, we have approximately $\xi \simeq \frac{c_2^4}{3c_2^2 + 2c_{12}^2}$ based on the results in Eqs. (2.3) - (2.5).

- (ii) $\mu^- \mu^+ \rightarrow \nu \bar{\nu} Z(\rightarrow \ell^- \ell^+) h_1(\rightarrow b\bar{b})$ and $\mu^- \mu^+ \rightarrow \ell^- \ell^+ Z(\rightarrow \ell^- \ell^+) h_1(\rightarrow b\bar{b})$, labeled “b2” with cross section σ_{b2} .
- (iii) $\mu^- \mu^+ \rightarrow \nu \bar{\nu} Z(\rightarrow \ell^- \ell^+) Z(\rightarrow jj)$ and $\mu^- \mu^+ \rightarrow \ell^- \ell^+ Z(\rightarrow \ell^- \ell^+) Z(\rightarrow jj)$, labeled “b3” with cross section σ_{b3} .
- (iv) $\mu^- \mu^+ \rightarrow b\bar{b} W^-(\rightarrow \bar{\nu} \ell^-) W^+(\rightarrow \nu \ell^+)$, labeled “b4” with cross section σ_{b4} .

The total cross section of backgrounds is defined as $\sigma_{\text{bkg}} \equiv \sigma_{b1} + \sigma_{b2} + \sigma_{b3} + \sigma_{b4}$.

Background events are generated with the same tools and settings as the signal. To maintain consistency, event yields are estimated from the `MadGraph5_aMC@NLO` (v3.6.2) [109] production cross sections. Note that b1 is a BSM background process, whose cross section depends on the parameters m_{h_2} , c_2 , and c_{12} ; while b2-b4 are all SM background processes, whose cross sections do not depend on the BSM parameters.

²In this paper, we only discuss the case $c_2, c_{12} > 0$ for simplify.

3.3 Analysis strategy

3.3.1 Pre-selection

Final-state leptons and b -jets are ordered by descending transverse momentum and labeled O_i ($i = 1, 2, \dots$), with $O \in \{\ell, b\text{-jet}\}$. We apply the following pre-selection cuts to select the target final state and reject background at the first stage:

- (i) Exactly two opposite-charge, same-flavor leptons, i.e. $N(\ell) = 2$ with $\ell = e, \mu$.
- (ii) Exactly two b -tagged jets, i.e. $N(j_b) = 2$.

Jets do not carry a well-defined electric charge; the so-called ‘‘jet charge’’ is an estimator and is not used here to require ‘‘opposite charges’’ for b -jets [124–126]. The second condition will miss the events in which two b -jets are not fully tagged, and include the events in which light jets are mis-tagged as two b -jets, as discussed above.

3.3.2 Reconstruction

In the signal topology, the heavy h_2 decays to one SM Higgs h_1 and one Z boson; subsequently $Z \rightarrow \ell^+\ell^-$ and $h_1 \rightarrow b\bar{b}$. We reconstruct the h_2 mass from the invariant mass of the $\ell^+\ell^-b\bar{b}$ system, $m_{b\bar{b}\ell-\ell^+}$; and the h_1 mass from the invariant mass of the two b jets, $m_{b\bar{b}}$. The two undetected energetic forward/backward objects (neutrinos or absorbed muons) form the invisible system, and we define its invariant mass as \cancel{m} , which captures the VBF kinematic features in both signal and some background processes. In our detailed study, we find that setting selection cuts on $m_{b\bar{b}}$ and $m_{b\bar{b}\ell-\ell^+}$ is enough to separate signal and background events, and thus \cancel{m} is only used as a tagging condition for VBF processes.

In this section, we choose two benchmark points: (i) $m_{h_2} = 700$ GeV with $\sqrt{s} = 3$ TeV, and (ii) $m_{h_2} = 3000$ GeV with $\sqrt{s} = 10$ TeV, to show how the selection cuts are set for the observables, $m_{b\bar{b}}$ and $m_{b\bar{b}\ell-\ell^+}$, together with the total cross sections for both signal and background after the selection cuts. Details for the other six benchmark points are put in the appendices.

In Fig. 3, we choose the benchmark point (i), and show the normalized distributions of $m_{b\bar{b}}$, $m_{b\bar{b}\ell-\ell^+}$, and \cancel{m} , for both signal and background processes after pre-selection. Based

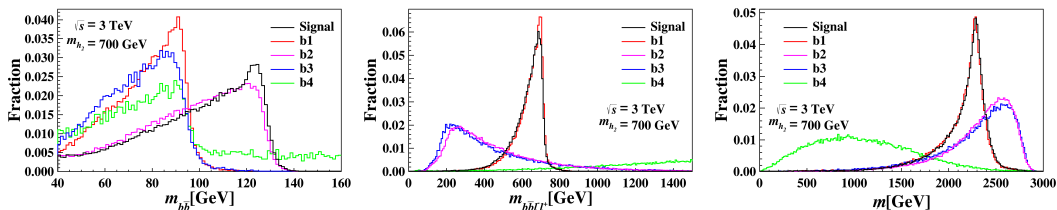


Figure 3: Normalized distributions of $m_{b\bar{b}}$ (left), $m_{b\bar{b}\ell-\ell^+}$ (middle), and \cancel{m} (right), for both signal and background processes after pre-selection ($m_{h_2} = 700$ GeV with $\sqrt{s} = 3$ TeV).

on the left plot, we choose the selection cut $100 \text{ GeV} \leq m_{b\bar{b}} \leq 140 \text{ GeV}$, which is effective

to suppress backgrounds b1, b3, and b4. In background b2, the $b\bar{b}$ -pairs also come from h_1 , meaning that its distribution should be similar to that of the signal process. Based on the middle plot, we choose the selection cut $640 \text{ GeV} \leq m_{b\bar{b}\ell-\ell^+} \leq 720 \text{ GeV}$ ³, which is effective to suppress backgrounds b2, b3, and b4. Since b1 is a BSM background which also comes from the h_2 decay, the $m_{b\bar{b}\ell-\ell^+}$ distribution in b1 should be similar to that of the signal process. If we perform these two selection cuts together, it is efficient to suppress all the four background processes. We also show the distribution of ηh distributions as a VBF tagging condition; however, it cannot provide further separation between the signal and background processes, after we set selection cuts on $m_{b\bar{b}}$ and $m_{b\bar{b}\ell-\ell^+}$. After selection cuts, we have the total cross sections for both signal and background processes as

$$\sigma_{\text{sig}} = 1.58\kappa \text{ (fb)}, \quad \text{and} \quad \sigma_{\text{bkg}} = (14\xi + 5.1) \times 10^{-3} \text{ (fb)}; \quad (3.6)$$

which can be used to predict the discovery potential of this process for given model parameters (c_2, c_{12}) and integrated luminosity L , with $m_{h_2} = 700 \text{ GeV}$.

In Fig. 4, we choose the benchmark point (ii), and show the normalized distributions of $m_{b\bar{b}}$, $m_{b\bar{b}\ell-\ell^+}$, and ηh , for both signal and background processes after pre-selection. Based

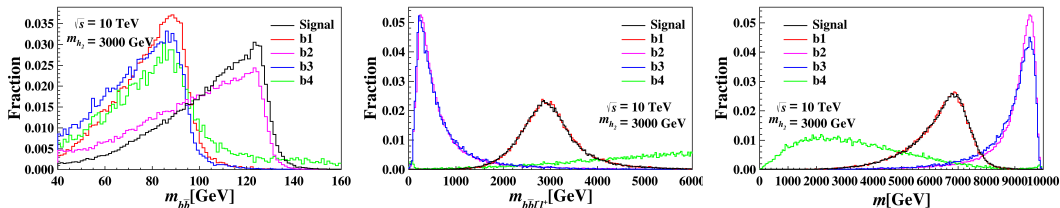


Figure 4: Normalized distributions of $m_{b\bar{b}}$ (left), $m_{b\bar{b}\ell-\ell^+}$ (middle), and ηh (right), for both signal and background processes after preselection ($m_{h_2} = 3000 \text{ GeV}$ with $\sqrt{s} = 10 \text{ TeV}$).

on the left plot, the distributions of $m_{b\bar{b}}$ for both signal and background processes are quite similar to those in the case of benchmark point (i), so thus we choose the selection cut $100 \text{ GeV} \leq m_{b\bar{b}} \leq 140 \text{ GeV}$ again. Based on the middle plot, it can be found that the signal peak is much wider than that for benchmark point (i), and we choose the selection cut $2400 \text{ GeV} \leq m_{b\bar{b}\ell-\ell^+} \leq 3400 \text{ GeV}$. Cuts on ηh in the right plot cannot provide further separation between signal and background processes after selection cuts on $m_{b\bar{b}}$ and $m_{b\bar{b}\ell-\ell^+}$, whose behavior is similar to that in benchmark point (i). After selection cuts, we have the total cross sections for both signal and background processes as

$$\sigma_{\text{sig}} = 1.13\kappa \text{ (fb)}, \quad \text{and} \quad \sigma_{\text{bkg}} = (17\xi + 7.07) \times 10^{-3} \text{ (fb)}. \quad (3.7)$$

³The minimal necessary width of the cut window, which relate closely to the dispersion in $m_{b\bar{b}\ell-\ell^+}$ distribution, is sensitive to both the energy smearing at detector level and the total width of h_2 (especially for large m_{h_2}), denoted as Γ_{h_2} , which is calculated in Eq. (2.7). In this work, all signal events are generated using the benchmark point $c_2 = c_{12} = 0.2$ leading to the largest allowed Γ_{h_2} , which ensures our search strategy works in the whole parameter region as we consider.

More details are shown in the appendices. For the other six benchmark points, we show the normalized distributions of $m_{b\bar{b}}$, $m_{b\bar{b}\ell-\ell^+}$, and $\eta\hbar$ in Appendix A. Following these distributions, we set the selection cuts on $m_{b\bar{b}}$ and $m_{b\bar{b}\ell-\ell^+}$ for all the eight benchmark points. The selection cuts on $m_{b\bar{b}}$ are the same for all the eight benchmark points, $100 \text{ GeV} \leq m_{b\bar{b}} \leq 140 \text{ GeV}$; while the selection cuts on $m_{b\bar{b}\ell-\ell^+}$ are sensitive to m_{h_2} , as shown in Table 1. For all the eight benchmark points, $\eta\hbar$ cannot be used to separate signal and background processes further after setting selection cuts on $m_{b\bar{b}}$ and $m_{b\bar{b}\ell-\ell^+}$, thus it is only used as VBF tagging.

m_{h_2} [GeV]	700	1000	700	1000
\sqrt{s} [TeV]	3	3	10	10
$m_{b\bar{b}\ell-\ell^+}$ Cut [GeV]	640 – 720	920 – 1020	640 – 720	920 – 1020
m_{h_2} [GeV]	1500	2000	3000	4500
\sqrt{s} [TeV]	10	10	10	10
$m_{b\bar{b}\ell-\ell^+}$ Cut [GeV]	1300 – 1600	1700 – 2200	2400 – 3400	3400 – 5400

Table 1: Selection cuts on $m_{b\bar{b}\ell-\ell^+}$ for all the eight benchmark points.

Following all the analysis procedure above, we show the cross sections for both signal and background processes for all the eight benchmark points, after each step (initial production, pre-selection cuts, and selection cuts), in Appendix B. For background processes, we show both σ_{b1-b4} separately and the total cross section σ_{bkg} . If $(c_2, c_{12}) \leq 0.2$, we have $\xi \simeq \frac{c_2^4}{3c_2^2 + 2c_{12}^2} \lesssim 1.3 \times 10^{-2}$, and thus for each benchmark point, the dominant background after selection cuts should be b2.

4 Results

The expected event numbers of signal and background processes after selection cuts are

$$N_{\text{sig}} = \sigma_{\text{sig}} L, \quad \text{and} \quad N_{\text{bkg}} = \sigma_{\text{bkg}} L, \quad (4.1)$$

where L is the integrated luminosity. The statistical significance is quantified through

$$\sigma_{\text{stat}} = \sqrt{2 \left[(N_{\text{sig}} + N_{\text{bkg}}) \ln \left(1 + \frac{N_{\text{sig}}}{N_{\text{bkg}}} \right) - N_{\text{sig}} \right]}, \quad (4.2)$$

which increases as $L^{1/2}$. Based on the analysis above, we present the expected discovery potential for CP violation in scalar sector at muon colliders with $\sqrt{s} = 3$ (10) TeV and the corresponding integrated luminosity $L = 0.9$ (10) ab^{-1} , in Figs. 5-6.

For MuC with $\sqrt{s} = 3$ TeV and corresponding integrated luminosity $L = 0.9 \text{ ab}^{-1}$, assuming both $(c_2, c_{12}) \lesssim 0.2$, CP violation in the scalar sector can be discovered at 5σ

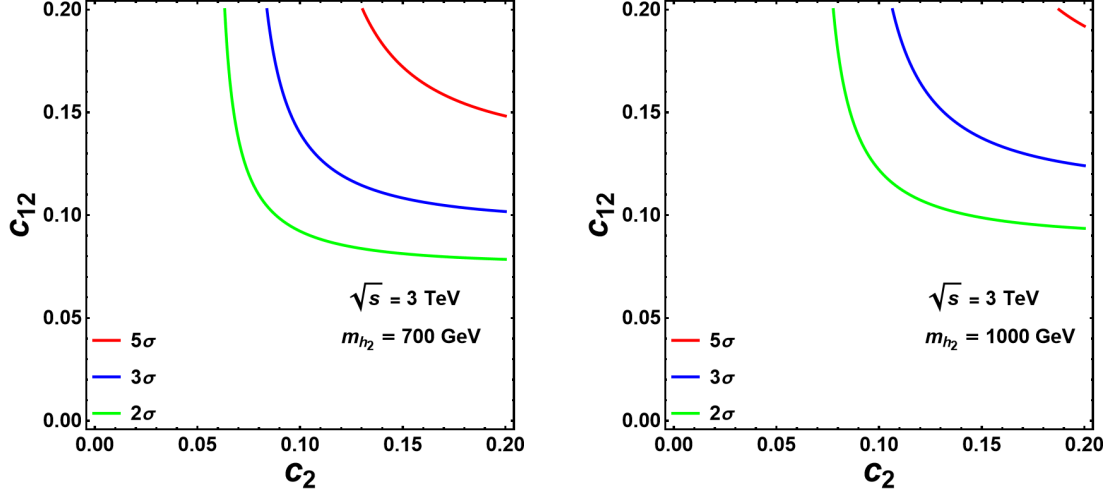


Figure 5: Expected discovery potential for significance for points in (c_2, c_{12}) -plane with $\sqrt{s} = 3$ TeV and $L = 0.9$ ab^{-1} . Benchmark points: $m_{h_2} \in \{700, 1000\}$ GeV. The colored lines correspond to the boundaries with expected 2σ (green), 3σ (blue), and 5σ (red) significances, respectively.

level up to $m_{h_2} \simeq 1$ TeV. For larger m_{h_2} , the cross section decreases quickly which leads to the weaker discovery potential. While for MuC with $\sqrt{s} = 10$ TeV and corresponding integrated luminosity $L = 10$ ab^{-1} , assuming both $(c_2, c_{12}) \lesssim 0.2$, CP violation in the scalar sector can be discovered at 5σ level up to $m_{h_2} \simeq 4.5$ TeV, because of the larger cross section and integrated luminosity. When $m_{h_2} \lesssim 3$ TeV, the discovery potential changes slowly, and the case with parameters $(c_2, c_{12}) \simeq 0.1$ can be discovered at 5σ level. The results show significant advantages for future MuC to test CP violation in the scalar sector, especially for the heavy h_2 scenario.

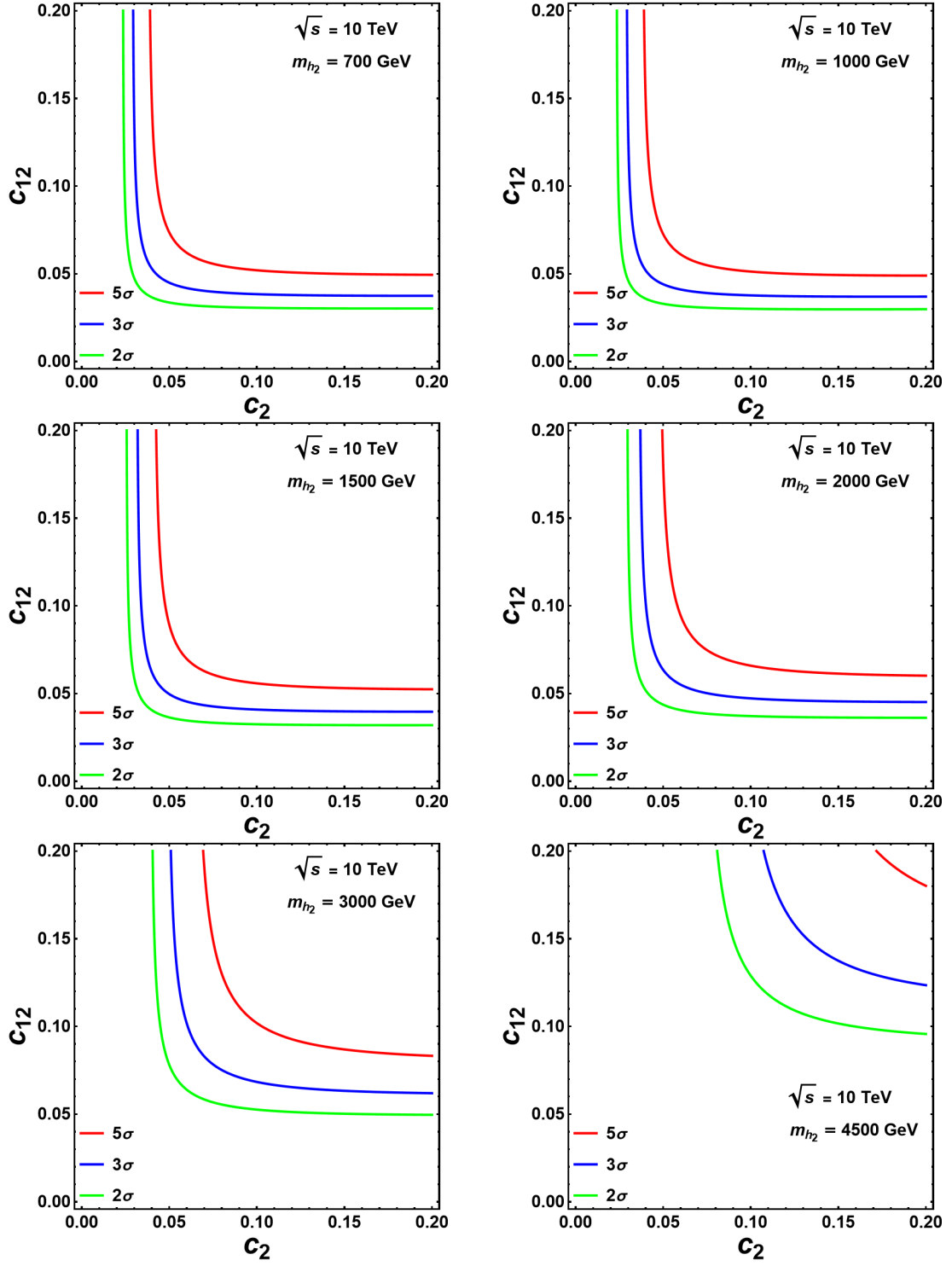


Figure 6: Expected discovery potential for significance for points in (c_2, c_{12}) -plane with $\sqrt{s} = 10$ TeV and $L = 10 \text{ ab}^{-1}$. Benchmark points: $m_{h_2} \in \{700, 1000, 1500, 2000, 3000, 4500\}$ GeV. The colored lines correspond to the boundaries with expected 2σ (green), 3σ (blue), and 5σ (red) significances, respectively.

5 Conclusions and discussions

We propose a model-independent strategy to test CP violation in an extended scalar sector at future muon colliders (MuC). The key observation is the existence of the single process

$$VV \rightarrow h_2 \rightarrow Zh_1, \quad (\text{with } V = W^\pm, Z). \quad (5.1)$$

It already requires both couplings $c_2 \neq 0$ and $c_{12} \neq 0$. Therefore, an observation of this channel is sufficient to establish CP violation in the scalar sector within the effective framework of Eq. (2.1). The absorbers to avoid BIB [115–118] lead to the same signal events coming from both W^+W^- - and ZZ -fusion processes, because the very forward/backward μ^\pm cannot be detected and thus behave as missing energy.

In our collider study, we focus on the clean final state $Z(\rightarrow \ell^+\ell^-)h_1(\rightarrow b\bar{b})$, exploited the reconstructed masses $m_{b\bar{b}\ell-\ell^+}$ and $m_{b\bar{b}}$, and used simple, robust selections to suppress backgrounds. After selection cuts, the dominant background is b2 for all benchmark points, while b1 is efficiently suppressed by $m_{b\bar{b}}$ cut, the smallness of ξ and $\text{Br}_{Z\rightarrow b\bar{b}}$. The sensitivity trends obtained at $\sqrt{s} = 3$ and 10 TeV (with the respective integrated luminosities $L = 0.9$ and 10 ab^{-1} used in Sec. 3) show that the VBF topology offers competitive discovery reach for a wide range of $m_{h_2} \sim \mathcal{O}(\text{TeV})$ at future MuC. Especially, for the $\sqrt{s} = 10$ TeV future MuC with $L = 10 \text{ ab}^{-1}$, $(c_2, c_{12}) \simeq 0.1$ (0.2) can be discovered at 5σ level up to a rather heavy $m_{h_2} \lesssim 3$ (4.5) TeV.

Our analysis targets the multi-TeV regime where VBF processes naturally benefit from the logarithmic enhancement of gauge boson radiation, making MuC an efficient “gauge boson collider”. The considered MuC parameters \sqrt{s} and L are consistent with current community roadmaps and interim reports for a staged MuC program [106, 108]. Within this context, the $VV \rightarrow h_2 \rightarrow Zh_1$ channel provides a direct handle on CP violation that is complementary to EDM constraints and to Yukawa-sector probes discussed in Sec. 1. Importantly, our selection is compatible with realistic machine–detector interface conditions at MuC, where forward/backward shielding against BIB [115–118] motivates restricted angular acceptance in the final states.

In this work, we focus on a general h_2 -interaction in Eq. (2.1), without assuming a complete model. Thus the method is universal for BSM models which contain one or more heavy scalar(s) with such type of interactions. As mentioned in Ref. [96], some CP-conserving neutral state h_2 may also interact with VV and Zh_1 at loop level. However, such scenarios are distinguishable from the case we discuss in this paper, because the loop-induced effective interactions always lead to small enough cross sections, corresponding to an effective $(c_2, c_{12}) \lesssim \mathcal{O}(10^{-2})$. That means our method at MuC is sufficient to confirm CP violation in the scalar sector.

In summary, observing $VV \rightarrow h_2 \rightarrow Zh_1$ with the selections outlined in this work would constitute compelling evidence for CP violation in the scalar sector; conversely, the non-observation can be translated into robust, model-independent bounds on the coupling combination (c_2, c_{12}) , providing a clear target for future MuC programs.

A Additional reconstruction distributions

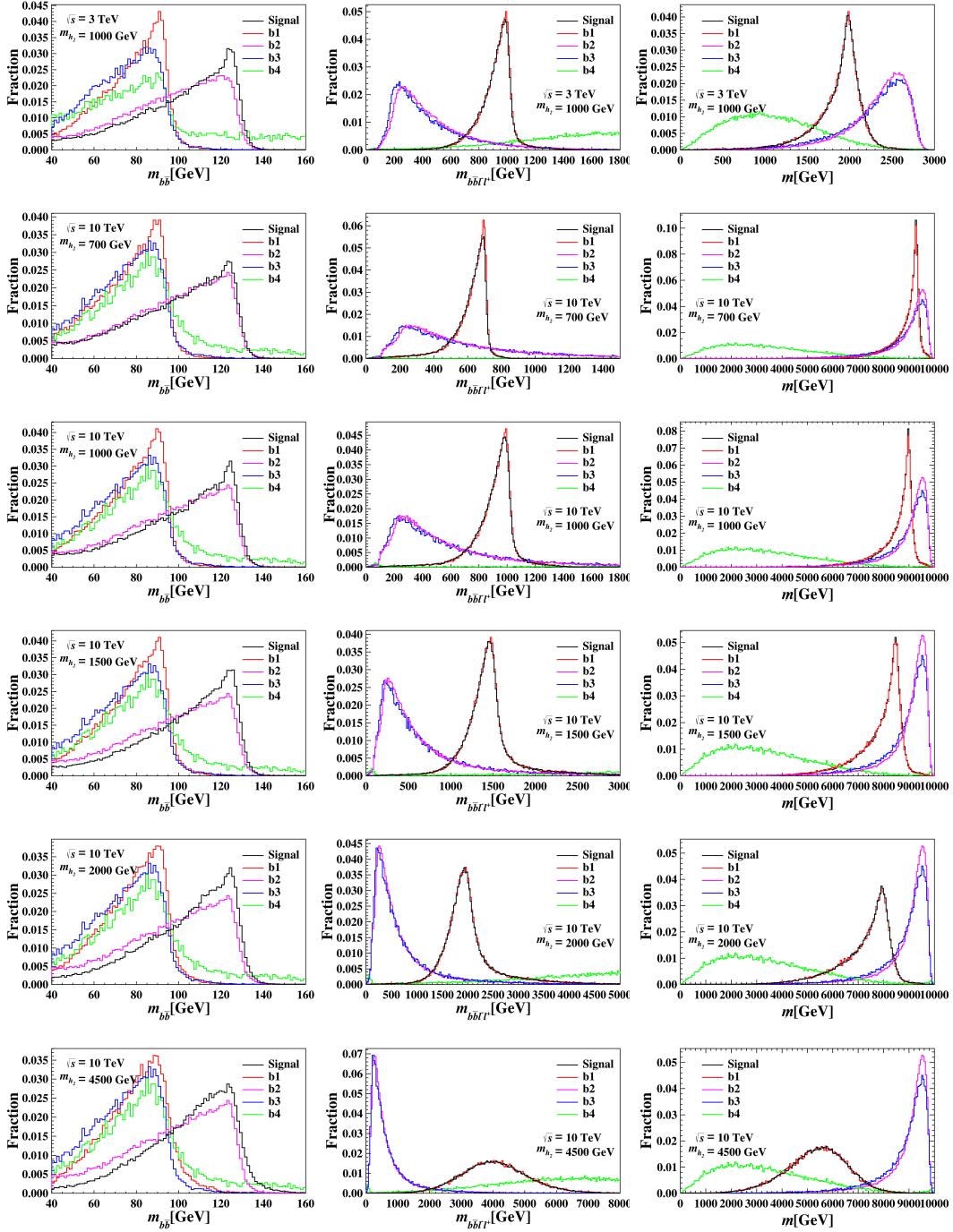


Figure 7: Normalized distributions of the observables $m_{b\bar{b}}$ (left), $m_{b\bar{b}\ell-\ell^+}$ (middle), and m_{η} (right), for all the other six benchmark points from top to bottom: $m_{h_2} = 1000$ GeV with $\sqrt{s} = 3$ TeV, and $m_{h_2} = 700, 1000, 1500, 2000, 4500$ GeV with $\sqrt{s} = 10$ TeV.

B Cross sections after each step

We show the cross sections for both signal and background processes after each step: initial production (denoted as “ini.”), pre-selection cuts (denoted as “pre-sel.”), and selection cuts (denoted as “sel.”). Results for the two benchmark points with $\sqrt{s} = 3$ TeV are shown in Table 2, and results for the six benchmark points with $\sqrt{s} = 10$ TeV are shown in Table 3

m_{h_2} [GeV]	cuts	σ_{sig} [fb]	σ_{bkg} [fb]	σ_{b1} [fb]	σ_{b2} [fb]	σ_{b3} [fb]	σ_{b4} [fb]
700	ini.	6.75κ	$8.16\xi+5.5$	8.16ξ	0.39	2.71	2.40
	pre-sel.	4.13κ	$1.12\xi+0.96$	1.12ξ	0.18	0.34	0.44
	sel.	1.58κ	$0.014\xi+0.0051$	0.014ξ	0.0045	0.00035	0.00025
1000	ini.	3.90κ	$4.68\kappa+5.5$	4.68κ	0.39	2.71	2.40
	pre-sel.	2.49κ	$0.72\xi+0.96$	0.72ξ	0.18	0.34	0.44
	sel.	0.86κ	$0.007\xi+0.0028$	0.007ξ	0.0022	0.00016	0.00044

Table 2: Cross sections for signal and background processes after each step (initial production, pre-selection cuts, and selection cuts) for benchmark points with $\sqrt{s} = 3$ TeV.

m_{h_2} [GeV]	cuts	σ_{sig} [fb]	σ_{bkg} [fb]	σ_{b1} [fb]	σ_{b2} [fb]	σ_{b3} [fb]	σ_{b4} [fb]
700	ini.	20.12κ	$24.18\xi+11.4$	24.18ξ	1.39	9.6	0.41
	pre-sel.	10.58κ	$3.24\xi+1.37$	3.24ξ	0.44	0.90	0.03
	sel.	3.74κ	$0.035\xi+0.00987$	0.035ξ	0.0092	0.00067	–
1000	ini.	16.15κ	$19.42\xi+11.4$	19.42ξ	1.39	9.60	0.41
	pre-sel.	9.30κ	$2.83\xi+1.37$	2.83ξ	0.44	0.90	0.03
	sel.	3.02κ	$0.038\xi+0.00625$	0.038ξ	0.0061	0.00015	–
1500	ini.	11.76κ	$14.13\xi+11.4$	14.13ξ	1.39	9.6	0.41
	pre-sel.	7.27κ	$2.19\xi+1.37$	2.19ξ	0.44	0.90	0.03
	sel.	2.96κ	$0.032\xi+0.00850$	0.032ξ	0.0084	0.00010	–
2000	ini.	8.70κ	$10.46\xi+11.4$	10.46ξ	1.39	9.6	0.41
	pre-sel.	5.40κ	$1.62\xi+1.37$	1.62ξ	0.44	0.90	0.03
	sel.	2.11κ	$0.025\xi+0.00752$	0.025ξ	0.0074	0.00012	–
3000	ini.	4.93κ	$5.93\xi+11.4$	5.93ξ	1.39	9.6	0.41
	pre-sel.	2.80κ	$0.85\xi+1.37$	0.85ξ	0.44	0.90	0.03
	sel.	1.13κ	$0.017\xi+0.00707$	0.017ξ	0.0069	0.00017	–
4500	ini.	1.98κ	$2.38\xi+11.4$	2.38ξ	1.39	9.6	0.41
	pre-sel.	0.67κ	$0.21\xi+1.37$	0.21ξ	0.44	0.90	0.03
	sel.	0.28κ	$0.007\xi+0.00493$	0.007ξ	0.0038	0.00083	0.00030

Table 3: Cross sections for signal and background processes after each step (initial production, pre-selection cuts, and section cuts) for benchmark points with $\sqrt{s} = 10$ TeV. “–” means this background process is negligible with $L = 10 \text{ ab}^{-1}$.

Acknowledgments

We thank Jin Sun and Rui Zhang for helpful discussions. Q.X.L. and Y.N.M. are supported by the National Natural Science Foundation of China under grant no. 12205227. K.W. is supported by the National Natural Science Foundation of China under grant no. 11905162, the Excellent Young Talents Program of the Wuhan University of Technology under grant no. 40122102, and the research program of the Wuhan University of Technology under grants no. 2020IB024 and 104972025KFYjc0101. The simulation and analysis work of this article was completed with the computational cluster provided by the Theoretical Physics Group at the Department of Physics, School of Physics and Mechanics, Wuhan University of Technology.

Note added. Following standard practice in high energy physics, authors are listed in strict alphabetical order by surname. This ordering should not be interpreted as indicating any ranking of contribution, seniority, or leadership. All authors contributed equally to this work.

References

- [1] J.H. Christenson, J.W. Cronin, V.L. Fitch and R. Turlay, *Evidence for the 2π Decay of the K_2^0 Meson*, *Phys. Rev. Lett.* **13** (1964) 138.
- [2] BELLE collaboration, *Observation of large CP violation in the neutral B meson system*, *Phys. Rev. Lett.* **87** (2001) 091802 [[hep-ex/0107061](#)].
- [3] BABAR collaboration, *Observation of CP violation in the B^0 meson system*, *Phys. Rev. Lett.* **87** (2001) 091801 [[hep-ex/0107013](#)].
- [4] BABAR collaboration, *Observation of direct CP violation in $B^0 \rightarrow K^+\pi^-$ decays*, *Phys. Rev. Lett.* **93** (2004) 131801 [[hep-ex/0407057](#)].
- [5] S. Khalil and S. Moretti, *Standard Model Phenomenology*, CRC Press (6, 2022).
- [6] PARTICLE DATA GROUP collaboration, *Review of particle physics*, *Phys. Rev. D* **110** (2024) 030001.
- [7] LHCb collaboration, *Observation of charge-parity symmetry breaking in baryon decays*, *Nature* **643** (2025) 1223 [[2503.16954](#)].
- [8] M. Kobayashi and T. Maskawa, *CP Violation in the Renormalizable Theory of Weak Interaction*, *Prog. Theor. Phys.* **49** (1973) 652.
- [9] N. Cabibbo, *Unitary Symmetry and Leptonic Decays*, *Phys. Rev. Lett.* **10** (1963) 531.
- [10] Y. Nir, *Cp violation in meson decays*, in *Les Houches*, vol. 84, pp. 79–145, Elsevier (2006).
- [11] HFLAV collaboration, *Averages of b-hadron, c-hadron, and τ -lepton properties as of 2021*, *Phys. Rev. D* **107** (2023) 052008 [[2206.07501](#)].
- [12] A.G. Cohen, D.B. Kaplan and A.E. Nelson, *Spontaneous baryogenesis at the weak phase transition*, *Phys. Lett. B* **263** (1991) 86.
- [13] A.G. Cohen, D.B. Kaplan and A.E. Nelson, *Progress in electroweak baryogenesis*, *Ann. Rev. Nucl. Part. Sci.* **43** (1993) 27 [[hep-ph/9302210](#)].
- [14] D.E. Morrissey and M.J. Ramsey-Musolf, *Electroweak baryogenesis*, *New J. Phys.* **14** (2012) 125003 [[1206.2942](#)].
- [15] T.D. Lee, *CP Nonconservation and Spontaneous Symmetry Breaking*, *Phys. Rept.* **9** (1974) 143.
- [16] S. Weinberg, *Gauge Theory of CP Violation*, *Phys. Rev. Lett.* **37** (1976) 657.
- [17] H. Georgi, *A Model of Soft CP Violation*, *Hadronic J.* **1** (1978) 155.
- [18] L. Bento, G.C. Branco and P.A. Parada, *A Minimal model with natural suppression of strong CP violation*, *Phys. Lett. B* **267** (1991) 95.
- [19] G.C. Branco, P.M. Ferreira, L. Lavoura, M.N. Rebelo, M. Sher and J.P. Silva, *Theory and phenomenology of two-Higgs-doublet models*, *Phys. Rept.* **516** (2012) 1 [[1106.0034](#)].

- [20] ACME collaboration, *Improved limit on the electric dipole moment of the electron*, *Nature* **562** (2018) 355.
- [21] T.S. Roussy et al., *An improved bound on the electron’s electric dipole moment*, *Science* **381** (2023) adg4084 [2212.11841].
- [22] C. Abel et al., *Measurement of the Permanent Electric Dipole Moment of the Neutron*, *Phys. Rev. Lett.* **124** (2020) 081803 [2001.11966].
- [23] B. Graner, Y. Chen, E. Lindahl and B. Heckel, *Reduced Limit on the Permanent Electric Dipole Moment of Hg199*, *Phys. Rev. Lett.* **116** (2016) 161601 [1601.04339].
- [24] M. Pospelov and A. Ritz, *Electric dipole moments as probes of new physics*, *Annals Phys.* **318** (2005) 119 [hep-ph/0504231].
- [25] J. Engel, M.J. Ramsey-Musolf and U. van Kolck, *Electric Dipole Moments of Nucleons, Nuclei, and Atoms: The Standard Model and Beyond*, *Prog. Part. Nucl. Phys.* **71** (2013) 21 [1303.2371].
- [26] N. Yamanaka, B.K. Sahoo, N. Yoshinaga, T. Sato, K. Asahi and B.P. Das, *Probing exotic phenomena at the interface of nuclear and particle physics with the electric dipole moments of diamagnetic atoms: A unique window to hadronic and semi-leptonic CP violation*, *Eur. Phys. J. A* **53** (2017) 54 [1703.01570].
- [27] M.S. Safronova, D. Budker, D. DeMille, D.F.J. Kimball, A. Derevianko and C.W. Clark, *Search for New Physics with Atoms and Molecules*, *Rev. Mod. Phys.* **90** (2018) 025008 [1710.01833].
- [28] T. Chupp, P. Fierlinger, M. Ramsey-Musolf and J. Singh, *Electric dipole moments of atoms, molecules, nuclei, and particles*, *Rev. Mod. Phys.* **91** (2019) 015001 [1710.02504].
- [29] Y. Yamaguchi and N. Yamanaka, *Large long-distance contributions to the electric dipole moments of charged leptons in the standard model*, *Phys. Rev. Lett.* **125** (2020) 241802 [2003.08195].
- [30] Y. Yamaguchi and N. Yamanaka, *Quark level and hadronic contributions to the electric dipole moment of charged leptons in the standard model*, *Phys. Rev. D* **103** (2021) 013001 [2006.00281].
- [31] A.W. El Kaffas, W. Khater, O.M. Ogreid and P. Osland, *Consistency of the two Higgs doublet model and CP violation in top production at the LHC*, *Nucl. Phys. B* **775** (2007) 45 [hep-ph/0605142].
- [32] S. Berge, W. Bernreuther and J. Ziethe, *Determining the CP parity of Higgs bosons at the LHC in their tau decay channels*, *Phys. Rev. Lett.* **100** (2008) 171605 [0801.2297].
- [33] J. Shu and Y. Zhang, *Impact of a CP Violating Higgs Sector: From LHC to Baryogenesis*, *Phys. Rev. Lett.* **111** (2013) 091801 [1304.0773].
- [34] Y.-n. Mao and S.-h. Zhu, *Lightness of Higgs boson and spontaneous CP violation in the Lee model*, *Phys. Rev. D* **90** (2014) 115024 [1409.6844].
- [35] C.-Y. Chen, S. Dawson and Y. Zhang, *Complementarity of LHC and EDMs for Exploring Higgs CP Violation*, *JHEP* **06** (2015) 056 [1503.01114].

- [36] V. Keus, S.F. King, S. Moretti and K. Yagyu, *CP Violating Two-Higgs-Doublet Model: Constraints and LHC Predictions*, *JHEP* **04** (2016) 048 [[1510.04028](#)].
- [37] G. Li, H.-R. Wang and S.-h. Zhu, *Probing CP-violating $h\bar{t}t$ coupling in $e^+e^- \rightarrow h\gamma$* , *Phys. Rev. D* **93** (2016) 055038 [[1506.06453](#)].
- [38] C. Shen and S.-h. Zhu, *Anomalous Higgs-top coupling pollution of the triple Higgs coupling extraction at a future high-luminosity electron-positron collider*, *Phys. Rev. D* **92** (2015) 094001 [[1504.05626](#)].
- [39] D. Fontes, J.C. Romão, R. Santos and J.P. Silva, *Large pseudoscalar Yukawa couplings in the complex 2HDM*, *JHEP* **06** (2015) 060 [[1502.01720](#)].
- [40] L. Bian and N. Chen, *Higgs pair productions in the CP-violating two-Higgs-doublet model*, *JHEP* **09** (2016) 069 [[1607.02703](#)].
- [41] Y.-n. Mao and S.-h. Zhu, *Lightness of a Higgs Boson and Spontaneous CP-violation in the Lee Model: An Alternative Scenario*, *Phys. Rev. D* **94** (2016) 055008 [[1602.00209](#)].
- [42] C.-Y. Chen, H.-L. Li and M. Ramsey-Musolf, *CP-Violation in the Two Higgs Doublet Model: from the LHC to EDMs*, *Phys. Rev. D* **97** (2018) 015020 [[1708.00435](#)].
- [43] Y.-n. Mao, *Spontaneous CP-violation in the Simplest Little Higgs Model and its Future Collider Tests: the Scalar Sector*, *Phys. Rev. D* **97** (2018) 075031 [[1703.10123](#)].
- [44] X. Chen, G. Li and X. Wan, *Probe CP violation in $H \rightarrow \gamma Z$ through forward-backward asymmetry*, *Phys. Rev. D* **96** (2017) 055023 [[1705.01254](#)].
- [45] X. Wan and Y.-K. Wang, *Probing the CP violating $H\gamma\gamma$ coupling using interferometry*, *Chin. Phys. C* **43** (2019) 073101 [[1712.00267](#)].
- [46] Y.-n. Mao, *Spontaneous CP-violation in the Simplest Little Higgs Model*, *PoS ICHEP2018* (2019) 003 [[1810.03854](#)].
- [47] K. Cheung, A. Jueid, Y.-n. Mao and S. Moretti, *Two-Higgs-doublet model with soft CP violation confronting electric dipole moments and colliders*, *Phys. Rev. D* **102** (2020) 075029 [[2003.04178](#)].
- [48] Q.-H. Cao, K.-P. Xie, H. Zhang and R. Zhang, *A New Observable for Measuring CP Property of Top-Higgs Interaction*, *Chin. Phys. C* **45** (2021) 023117 [[2008.13442](#)].
- [49] D. Azevedo, R. Capucha, E. Gouveia, A. Onofre and R. Santos, *Light Higgs searches in $t\bar{t}\phi$ production at the LHC*, *JHEP* **04** (2021) 077 [[2012.10730](#)].
- [50] D. Azevedo, R. Capucha, A. Onofre and R. Santos, *Scalar mass dependence of angular variables in $t\bar{t}\phi$ production*, *JHEP* **06** (2020) 155 [[2003.09043](#)].
- [51] S. Antusch, O. Fischer, A. Hammad and C. Scherb, *Testing CP Properties of Extra Higgs States at the HL-LHC*, *JHEP* **03** (2021) 200 [[2011.10388](#)].
- [52] S. Kanemura, M. Kubota and K. Yagyu, *Testing aligned CP-violating Higgs sector at future lepton colliders*, *JHEP* **04** (2021) 144 [[2101.03702](#)].
- [53] I. Low, N.R. Shah and X.-P. Wang, *Higgs alignment and novel CP-violating observables in two-Higgs-doublet models*, *Phys. Rev. D* **105** (2022) 035009 [[2012.00773](#)].
- [54] K. Enomoto, S. Kanemura and Y. Mura, *Electroweak baryogenesis in aligned two Higgs doublet models*, *JHEP* **01** (2022) 104 [[2111.13079](#)].

- [55] K. Enomoto, S. Kanemura and Y. Mura, *New benchmark scenarios of electroweak baryogenesis in aligned two Higgs double models*, *JHEP* **09** (2022) 121 [[2207.00060](#)].
- [56] J. Liu, Y. Nakai, Y. Shigekami and M. Song, *Probing CP violation in dark sector through the electron electric dipole moment*, *JHEP* **02** (2024) 082 [[2312.03340](#)].
- [57] K. Cheung, Y.-n. Mao, S. Moretti and R. Zhang, *Testing CP-violation in a heavy Higgs sector at CLIC*, *Eur. Phys. J. C* **85** (2025) 700 [[2304.04390](#)].
- [58] W.-S. Hou, G. Kumar and S. Teunissen, *Discovery prospects for electron and neutron electric dipole moments in the general two Higgs doublet model*, *Phys. Rev. D* **109** (2024) L011703 [[2308.04841](#)].
- [59] R. Boto, L. Lourenco, J.C. Romão and J.P. Silva, *Large pseudoscalar Yukawa couplings in the complex 3HDM*, *JHEP* **11** (2024) 106 [[2407.19856](#)].
- [60] T. Biekötter, D. Fontes, M. Mühlleitner, J.C. Romão, R. Santos and J.a.P. Silva, *Impact of new experimental data on the C2HDM: the strong interdependence between LHC Higgs data and the electron EDM*, *JHEP* **05** (2024) 127 [[2403.02425](#)].
- [61] K. Enomoto, S. Kanemura and S. Taniguchi, *The electric dipole moment in a model for neutrino mass, dark matter and baryon asymmetry of the Universe*, *JHEP* **06** (2025) 036 [[2403.13613](#)].
- [62] M. Aiko, M. Endo, S. Kanemura and Y. Mura, *Electroweak baryogenesis in 2HDM without EDM cancellation*, *JHEP* **07** (2025) 236 [[2504.07705](#)].
- [63] J.M. Dávila, A. Karan, E. Passemar, A. Pich and L. Vale Silva, *The Electric Dipole Moment of the electron in the decoupling limit of the aligned two-Higgs doublet model*, *JHEP* **10** (2025) 053 [[2504.16700](#)].
- [64] R. Boto, J.A.C. Matos, J.C. Romão and J.P. Silva, *Surveying the complex three Higgs doublet model with Machine Learning*, [2510.02445](#).
- [65] ATLAS collaboration, *Observation of a new particle in the search for the Standard Model Higgs boson with the ATLAS detector at the LHC*, *Phys. Lett. B* **716** (2012) 1 [[1207.7214](#)].
- [66] CMS collaboration, *Observation of a New Boson at a Mass of 125 GeV with the CMS Experiment at the LHC*, *Phys. Lett. B* **716** (2012) 30 [[1207.7235](#)].
- [67] ATLAS, CMS collaboration, *Combined Measurement of the Higgs Boson Mass in pp Collisions at $\sqrt{s} = 7$ and 8 TeV with the ATLAS and CMS Experiments*, *Phys. Rev. Lett.* **114** (2015) 191803 [[1503.07589](#)].
- [68] C.R. Schmidt and M.E. Peskin, *A Probe of CP violation in top quark pair production at hadron supercolliders*, *Phys. Rev. Lett.* **69** (1992) 410.
- [69] G. Mahlon and S.J. Parke, *Angular correlations in top quark pair production and decay at hadron colliders*, *Phys. Rev. D* **53** (1996) 4886 [[hep-ph/9512264](#)].
- [70] E. Asakawa and K. Hagiwara, *Probing the CP nature of the Higgs bosons by t anti-t production at photon linear colliders*, *Eur. Phys. J. C* **31** (2003) 351 [[hep-ph/0305323](#)].
- [71] P.S. Bhupal Dev, A. Djouadi, R.M. Godbole, M.M. Muhlleitner and S.D. Rindani, *Determining the CP properties of the Higgs boson*, *Phys. Rev. Lett.* **100** (2008) 051801 [[0707.2878](#)].

- [72] X.-G. He, G.-N. Li and Y.-J. Zheng, *Probing Higgs boson CP Properties with $t\bar{t}H$ at the LHC and the 100 TeV pp collider*, *Int. J. Mod. Phys. A* **30** (2015) 1550156 [[1501.00012](#)].
- [73] F. Boudjema, R.M. Godbole, D. Guadagnoli and K.A. Mohan, *Lab-frame observables for probing the top-Higgs interaction*, *Phys. Rev.* **D92** (2015) 015019 [[1501.03157](#)].
- [74] M.R. Buckley and D. Goncalves, *Boosting the Direct CP Measurement of the Higgs-Top Coupling*, *Phys. Rev. Lett.* **116** (2016) 091801 [[1507.07926](#)].
- [75] K. Hagiwara, K. Ma and H. Yokoya, *Probing CP violation in e^+e^- production of the Higgs boson and toponia*, *JHEP* **06** (2016) 048 [[1602.00684](#)].
- [76] S. Amor Dos Santos et al., *Probing the CP nature of the Higgs coupling in $t\bar{t}h$ events at the LHC*, *Phys. Rev. D* **96** (2017) 013004 [[1704.03565](#)].
- [77] D. Azevedo, A. Onofre, F. Filthaut and R. Goncalo, *CP tests of Higgs couplings in $t\bar{t}h$ semileptonic events at the LHC*, *Phys. Rev. D* **98** (2018) 033004 [[1711.05292](#)].
- [78] W. Bernreuther, L. Chen, I. García, M. Perelló, R. Poeschl, F. Richard et al., *CP-violating top quark couplings at future linear e^+e^- colliders*, *Eur. Phys. J. C* **78** (2018) 155 [[1710.06737](#)].
- [79] K. Hagiwara, H. Yokoya and Y.-J. Zheng, *Probing the CP properties of top Yukawa coupling at an e^+e^- collider*, *JHEP* **02** (2018) 180 [[1712.09953](#)].
- [80] K. Ma, *Enhancing CP Measurement of the Yukawa Interactions of Top-Quark at e^-e^+ Collider*, *Phys. Lett. B* **797** (2019) 134928 [[1809.07127](#)].
- [81] M. Cepeda et al., *Report from Working Group 2: Higgs Physics at the HL-LHC and HE-LHC*, *CERN Yellow Rep. Monogr.* **7** (2019) 221 [[1902.00134](#)].
- [82] D.A. Faroughy, J.F. Kamenik, N. Košnik and A. Smolkovič, *Probing the CP nature of the top quark Yukawa at hadron colliders*, *JHEP* **02** (2020) 085 [[1909.00007](#)].
- [83] V. Barger, K. Hagiwara and Y.-J. Zheng, *CP-violating top-Higgs coupling in SMEFT*, *Phys. Lett. B* **850** (2024) 138547 [[2310.10852](#)].
- [84] M.E. Cassidy, Z. Dong, K. Kong, I.M. Lewis, Y. Zhang and Y.-J. Zheng, *Probing the CP structure of the top quark Yukawa at the future muon collider*, *JHEP* **05** (2024) 176 [[2311.07645](#)].
- [85] W. Esmail, A. Hammad, A. Jueid and S. Moretti, *Boosting probes of CP violation in the top Yukawa coupling with Deep Learning*, [2405.16499](#).
- [86] A. Hammad and A. Jueid, *Progress in CP violating top-Higgs coupling at the LHC with Machine Learning*, [2504.11791](#).
- [87] K. Desch, A. Imhof, Z. Was and M. Worek, *Probing the CP nature of the Higgs boson at linear colliders with tau spin correlations: The Case of mixed scalar - pseudoscalar couplings*, *Phys. Lett. B* **579** (2004) 157 [[hep-ph/0307331](#)].
- [88] R. Harnik, A. Martin, T. Okui, R. Primulando and F. Yu, *Measuring CP Violation in $h \rightarrow \tau^+\tau^-$ at Colliders*, *Phys. Rev. D* **88** (2013) 076009 [[1308.1094](#)].
- [89] S. Berge, W. Bernreuther and H. Spiesberger, *Higgs CP properties using the τ decay modes at the ILC*, *Phys. Lett. B* **727** (2013) 488 [[1308.2674](#)].

- [90] S. Berge, W. Bernreuther and S. Kirchner, *Determination of the Higgs CP-mixing angle in the tau decay channels at the LHC including the Drell–Yan background*, *Eur. Phys. J. C* **74** (2014) 3164 [[1408.0798](#)].
- [91] S. Berge, W. Bernreuther and S. Kirchner, *Prospects of constraining the Higgs boson’s CP nature in the tau decay channel at the LHC*, *Phys. Rev. D* **92** (2015) 096012 [[1510.03850](#)].
- [92] A. Askew, P. Jaiswal, T. Okui, H.B. Prosper and N. Sato, *Prospect for measuring the CP phase in the $h\tau\tau$ coupling at the LHC*, *Phys. Rev. D* **91** (2015) 075014 [[1501.03156](#)].
- [93] R. Józefowicz, E. Richter-Was and Z. Was, *Potential for optimizing the Higgs boson CP measurement in $H \rightarrow \tau\tau$ decays at the LHC including machine learning techniques*, *Phys. Rev. D* **94** (2016) 093001 [[1608.02609](#)].
- [94] K. Hagiwara, K. Ma and S. Mori, *Probing CP violation in $h \rightarrow \tau^-\tau^+$ at the LHC*, *Phys. Rev. Lett.* **118** (2017) 171802 [[1609.00943](#)].
- [95] S. Kanemura, M. Takeuchi and K. Yagyu, *Probing double-aligned two-Higgs-doublet models at the LHC*, *Phys. Rev. D* **105** (2022) 115001 [[2112.13679](#)].
- [96] G. Li, Y.-n. Mao, C. Zhang and S.-h. Zhu, *Testing CP violation in the scalar sector at future e^+e^- colliders*, *Phys. Rev. D* **95** (2017) 035015 [[1611.08518](#)].
- [97] A. Mendez and A. Pomarol, *Signals of CP violation in the Higgs sector*, *Phys. Lett. B* **272** (1991) 313.
- [98] R. Capucha, Á. Lozano-Onrubia, L. Merlo, J.M. No and R. Santos, *V-Associated Production & Vector Boson Fusion as an LHC Signature of CP Violation*, [2507.05942](#).
- [99] CEPC STUDY GROUP collaboration, *CEPC Conceptual Design Report: Volume 2 - Physics & Detector*, [1811.10545](#).
- [100] CEPC STUDY GROUP collaboration, *CEPC Technical Design Report: Accelerator*, *Radiat. Detect. Technol. Methods* **8** (2024) 1 [[2312.14363](#)].
- [101] S. Antusch et al., *New Physics Search at the CEPC: a General Perspective*, [2505.24810](#).
- [102] J.P. Delahaye, M. Diemoz, K. Long, B. Mansoulié, N. Pastrone, L. Rivkin et al., *Muon Colliders*, [1901.06150](#).
- [103] C. Aime et al., *Muon Collider Physics Summary*, [2203.07256](#).
- [104] K.M. Black et al., *Muon Collider Forum report*, *JINST* **19** (2024) T02015 [[2209.01318](#)].
- [105] C. Accettura et al., *Towards a muon collider*, *Eur. Phys. J. C* **83** (2023) 864 [[2303.08533](#)].
- [106] INTERNATIONAL MUON COLLIDER collaboration, *Interim report for the International Muon Collider Collaboration (IMCC)*, *CERN Yellow Rep. Monogr.* **2/2024** (2024) 176 [[2407.12450](#)].
- [107] INTERNATIONAL MUON COLLIDER collaboration, *The Muon Collider*, [2504.21417](#).
- [108] A. Abdelhamid et al., *United states muon collider community white paper*, [2503.23695](#).
- [109] J. Alwall, R. Frederix, S. Frixione, V. Hirschi, F. Maltoni, O. Mattelaer et al., *The automated computation of tree-level and next-to-leading order differential cross sections, and their matching to parton shower simulations*, *JHEP* **07** (2014) 079 [[1405.0301](#)].

- [110] A. Djouadi, *The Anatomy of electro-weak symmetry breaking. I: The Higgs boson in the standard model*, *Phys. Rept.* **457** (2008) 1 [[hep-ph/0503172](#)].
- [111] A. Djouadi, *The Anatomy of electro-weak symmetry breaking. II. The Higgs bosons in the minimal supersymmetric model*, *Phys. Rept.* **459** (2008) 1 [[hep-ph/0503173](#)].
- [112] A. Alloul, N.D. Christensen, C. Degrande, C. Duhr and B. Fuks, *FeynRules 2.0 - A complete toolbox for tree-level phenomenology*, *Comput. Phys. Commun.* **185** (2014) 2250 [[1310.1921](#)].
- [113] C. Bierlich et al., *A comprehensive guide to the physics and usage of PYTHIA 8.3*, *SciPost Phys. Codeb.* **2022** (2022) 8 [[2203.11601](#)].
- [114] DELPHES 3 collaboration, *DELPHES 3, A modular framework for fast simulation of a generic collider experiment*, *JHEP* **02** (2014) 057 [[1307.6346](#)].
- [115] N.V. Mokhov and S.I. Striganov, *Detector Background at Muon Colliders*, *Phys. Procedia* **37** (2012) 2015 [[1204.6721](#)].
- [116] N.V. Mokhov, S.I. Striganov and I.S. Tropin, *Reducing Backgrounds in the Higgs Factory Muon Collider Detector*, in *5th International Particle Accelerator Conference*, pp. 1081–1083, 6, 2014, DOI [[1409.1939](#)].
- [117] V. Di Benedetto, C. Gatto, A. Mazzacane, N.V. Mokhov, S.I. Striganov and N.K. Terentiev, *A Study of Muon Collider Background Rejection Criteria in Silicon Vertex and Tracker Detectors*, *JINST* **13** (2018) P09004 [[1807.00074](#)].
- [118] N. Bartosik et al., *Preliminary Report on the Study of Beam-Induced Background Effects at a Muon Collider*, [1905.03725](#).
- [119] M. Cacciari, G.P. Salam and G. Soyez, *FastJet User Manual*, *Eur. Phys. J. C* **72** (2012) 1896 [[1111.6097](#)].
- [120] M. Boronat, I. Garcia and M. Vos, *A new jet reconstruction algorithm for lepton colliders*, [1404.4294](#).
- [121] M. Boronat et al., *Jet reconstruction at high-energy lepton colliders*, [1607.05039](#).
- [122] CLICDP collaboration, *A detector for CLIC: main parameters and performance*, [1812.07337](#).
- [123] ATLAS collaboration, *Search for heavy resonances decaying into a pair of Z bosons in the $\ell^+\ell^-\ell'^+\ell'^-$ and $\ell^+\ell^-\nu\bar{\nu}$ final states using 139 fb^{-1} of proton–proton collisions at $\sqrt{s} = 13\text{ TeV}$ with the ATLAS detector*, *Eur. Phys. J. C* **81** (2021) 332 [[2009.14791](#)].
- [124] ATLAS collaboration, *Measurement of jet charge in dijet events from $\sqrt{s}=8\text{ TeV}$ pp collisions with the ATLAS detector*, *Phys. Rev. D* **93** (2016) 052003 [[1509.05190](#)].
- [125] CMS collaboration, *Measurements of jet charge with dijet events in pp collisions at $\sqrt{s} = 8\text{ TeV}$* , *JHEP* **10** (2017) 131 [[1706.05868](#)].
- [126] R. Kogler et al., *Jet Substructure at the Large Hadron Collider: Experimental Review*, *Rev. Mod. Phys.* **91** (2019) 045003 [[1803.06991](#)].